



Short communication

Direct ethanol solid oxide fuel cell operating in gradual internal reforming

S.D. Nobrega^a, M.V. Galesco^b, K. Girona^b, D.Z. de Florio^c, M.C. Steil^b, S. Georges^b, F.C. Fonseca^{a,*}^a Instituto de Pesquisas Energéticas e Nucleares, IPEN-CNEN/SP, São Paulo, SP 05508-000, Brazil^b Laboratoire d'Electrochimie et de Physicochimie des Matériaux et des Interfaces, UMR 5279, CNRS-Grenoble INP, UJF, 38400 St. Martin d'Hères, France^c Universidade Federal do ABC, Santo André, SP 09210-170, Brazil

ARTICLE INFO

Article history:

Received 6 January 2012

Received in revised form

27 March 2012

Accepted 30 March 2012

Available online 20 April 2012

Keywords:

Solid oxide fuel cell

Ethanol

Catalytic layer

Gradual internal reforming

ABSTRACT

An electrolyte supported solid oxide fuel cell (SOFC) using standard electrodes, doped-lanthanum manganite cathode and Ni-cermet anode, was operated with direct (anhydrous) ethanol for more than 100 h, delivering essentially the same power output as running on hydrogen. A ceria-based layer provides the catalytic activity for the gradual internal reforming, which uses the steam formed by the electrochemical oxidation of hydrogen for the decomposition of ethanol. Such a concept opens up the way for multi-fuel SOFCs using standard components and a catalytic layer.

© 2012 Elsevier B.V. Open access under the [Elsevier OA license](#).

1. Introduction

Solid Oxide Fuel Cells (SOFCs) are emerging as a clean and efficient power generation technology. Such ceramic fuel cells have the highest potential efficiency for conversion of chemical fuels directly into electrical power [1]. Due to the high operating temperatures, typically $\geq 800^\circ\text{C}$, SOFCs have the potential for operating with various fuels in addition to hydrogen. Although such a remarkable feature ranks SOFC in a strategic position amongst other fuel cell technologies, the effective use of carbon containing fuels is severely hindered due to limitations of the traditionally used Ni/yttria-stabilized zirconia (Ni/YSZ) cermet anode [2]. When carbon containing fuels are directly fed to the SOFC the use of the Ni-based cermet is impracticable due to catastrophic carbon deposition and subsequent anode collapse.

Amongst alternative SOFC fuels, hydrocarbons, such as methane, have been used provided that sufficient water or other reforming agent like CO_2 or O_2 is added to avoid carbon deposition [3]. However, such addition dilutes the fuel, lowers the SOFC efficiency by decreasing the Nernst potential, adds complexity to the system and strongly affects the cell durability. The direct oxidation of hydrocarbon fuels was successfully demonstrated in Cu-ceria

cermets [4]; however, some issues mainly related to the processing have held back a more widespread application of such anodes. Therefore, the efficient use of carbon containing fuels remains as one of the most relevant issues in SOFC development.

Sugar cane derived bioethanol has been proved as an efficient and competitive renewable fuel that powers vehicles, promoting a significant reduction of pollutants from combustion [5]. Such a biofuel adds all the advantages of liquid fuels and yet has a rather high energy density. The estimated losses for the conversion of the energy content in sugar glucose to ethanol and then reacting it to yield hydrogen is below 20% [6]. Hence, such a renewable fuel is a very attractive hydrogen source for fuel cells.

Previous studies on ethanol fueled SOFC were mostly based on internal steam reforming [7–11] or have used non-standard anodes [12–14]. Few studies investigated the short term stability, but essentially all previously reported data have shown a significant decrease of the fuel cell performance when hydrogen is switched to ethanol. In the present study, the SOFC operation is ensured by the gradual internal reforming. Gradual internal reforming is based on a local coupling between steam reforming of the fuel that occurs in a catalytic layer and hydrogen electrochemical oxidation, which occurs at the electrode triple-phase boundary [15]. Thus, the water released by the electrochemical oxidation of hydrogen at the anode (1) is used for the steam reforming of the ethanol (2) in a catalytic layer deposited over the anode [15–18]. Under ideal conditions, such a mechanism can be represented by the reactions:

* Corresponding author. Tel./fax: +55 11 31339282.

E-mail address: fconseca@ipen.br (F.C. Fonseca).



Therefore, provided that an efficient catalyst is used, reactions (1) and (2) sustain each other and ensure fuel cell operation. The gradual internal reforming has been previously theoretically studied and experimentally demonstrated for dry methane [15–18]. The present study extends this concept to ethanol.

2. Experimental

Electrolyte supported SOFCs were fabricated using the standard single cell components, as described elsewhere [17,18]. Yttria-stabilized zirconia (YSZ) cylindrical supports, 1 mm thick and 56 mm diameter, were produced by pressing and sintering (1450 °C for 2 h) commercial (Tosoh TZ8Y) powder, followed by a rectifying step in diamond tool to ensure dimensional accuracy. The deposition of the electrodes was done by spray coating. Homemade NiO/YSZ (tailored to 40 vol.% Ni after reduction) anode precursor and commercial $\text{La}_{0.8}\text{Sr}_{0.2}\text{MnO}_{3-\delta}$ (LSM, Praxair) cathode were used to prepare ethanol-based suspensions [17]. Electrodes deposition followed the sequence: i) anode deposition and sintering at 1400 °C for 1 h; ii) functional cathode YSZ/LSM (50/50 wt.%) composite layer deposition; and iii) current collector LSM cathode deposition and sintering at 1100 °C. Final thickness of the anode and cathode was 60 and 70 μm, respectively, and the active electrode area was 13.8 cm².

Because of both the good catalytic activity and the compatibility with SOFC components, a ceria-based catalytic layer was selected to be deposited onto the anode. The catalytic coating was formed by two layers: i) a 80 μm thick layer of 10 mol% gadolinia doped-ceria (CGO, Praxair, specific surface area 40.9 m² g⁻¹); and ii) a 20 μm thick layer of CGO with 0.1 wt.% of Ir. The Ir/CGO catalyst was prepared by impregnation of iridium (III) acetylacetonate (Alfa Aesar) in a toluene solution of CGO [19]. The ceria-based layers were deposited onto the anode following the same procedure described for electrodes deposition, and annealed at 900 °C in air.

The single cell was set up in a homemade test bench comprised of two alumina tubes (anode and cathode side) with a third external concentric alumina tube in which a guard atmosphere of Ar was flown [17]. Current collection on the cathode side was made by a gold grid, whilst in the anode side a special design using gold wire and paste assured electrical contact between the anode and terminal leads, as detailed elsewhere [17,18]. Current and potential monitoring was made by gold leads in a four wire configuration for independent current and voltage measurements. Fuel cell tests were initially performed under H₂ (60%) balanced with Ar with 4 L h⁻¹ total flow. After steady operation under H₂ at 860 °C, the fuel was switched to anhydrous ethanol. Ethanol was kept in a thermal bath with controlled temperature and carried by N₂ at 4 L h⁻¹ total flow rate. Gas flow rates were set by calibrated mass flowmeters (Brooks). Electrochemical impedance spectroscopy (EIS) and polarization vs. time measurements were performed by an Autolab PGSTAT128N potentiostat associated with a BSTR10A current booster. A variable resistor bench connected in series with the fuel cell was used for polarization curve determination.

3. Results and discussion

After anode reduction, a stable OCV of 1.25 V was measured at 860 °C. The SOFC performance was first evaluated in H₂. Fig. 1 presents the EIS diagrams taken at the OCV (Fig. 1a) and the

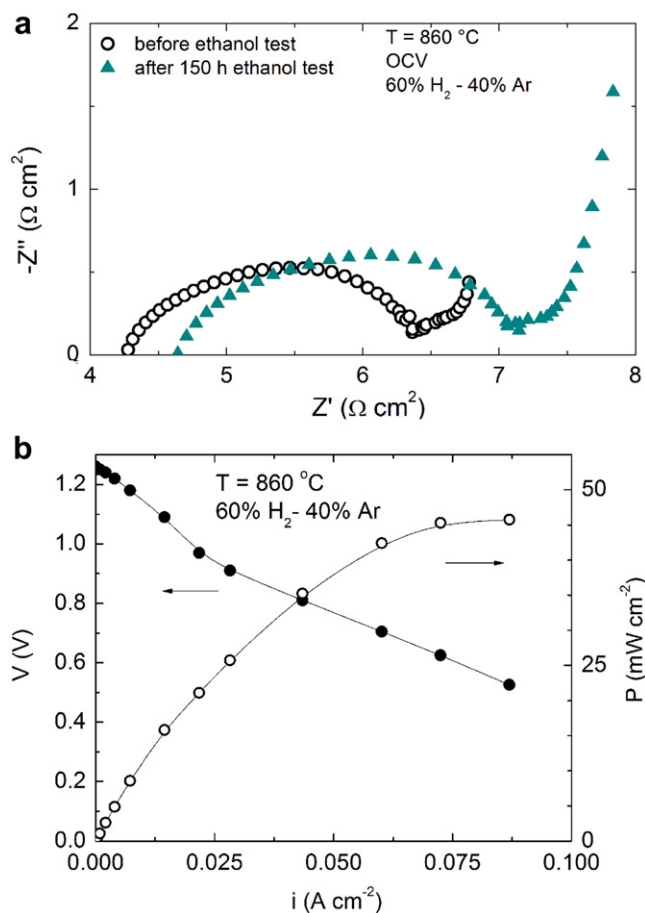


Fig. 1. (a) Impedance diagrams and (b) polarization curves of single SOFC with ceria-based catalytic layer running on H₂.

corresponding polarization curves (Fig. 1b) obtained at 860 °C. The EIS diagram exhibited convoluted contributions with a polarization resistance of ~2 Ω cm² and a supplementary low frequency tail, attributed to an additional diffusion resistance in the porous, but relatively thick (100 μm) catalytic layer. Nonetheless, such low frequency component was considerably less pronounced in EIS data taken under cell polarization at 0.7 V during ethanol operation, as displayed in Fig. 2. The polarization curves (Fig. 1b) exhibited a small deviation from linearity at low current density (*i*), suggesting an activation polarization component. The main polarization contribution has been associated to cathodic activation, as inferred from previously reported 5-electrode EIS measurements carried out in similar single cells [18]. Nevertheless, the rather linear curves at high *i* indicated that the main polarization component in the investigated current range was the ohmic loss. Indeed, the ohmic drop calculated from the high *i* portion of the polarization curve was consistent with the total resistance (~6.5 Ω cm²) of the EIS data. Such a result is directly related to the thick supporting electrolyte, which limited the maximum power densities to ~45 mW cm⁻² at *i* = 0.087 A cm⁻² and 0.5 V. Although the single cells used in the present study were not optimized for high power output, previous reports of SOFCs with similar anode configuration with a catalytic layer showed high power outputs (~1 W cm⁻²) running on H₂, indicating that the performance of such anode configuration is not intrinsically limited [20,21].

In order to investigate the stability in direct ethanol, the operation of the cell was initiated at 0.7 V in H₂ and the delivered *i* was recorded as a function of time, as shown in Fig. 2. After a steady

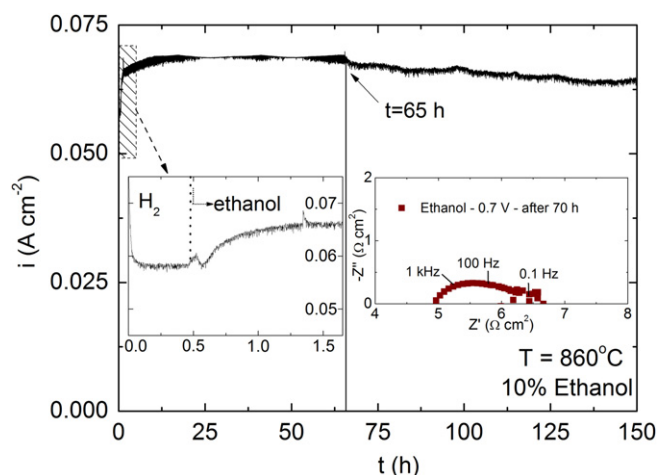


Fig. 2. Potentiostatic test at 0.7 V of the single SOFC containing a ceria-based catalytic layer under anhydrous ethanol. The left side inset shows the expanded shaded area, showing the initial hours of the test when hydrogen was changed to ethanol, as indicated by the dotted line. The right side inset shows the impedance measurement at 0.7 V performed in ethanol after 70 h of operation.

operation in H_2 was attained ($t \sim 0.5$ h), the anodic atmosphere was switched to anhydrous ethanol, ensuring a constant fuel supply to maintain the current density and steam release. The flow rates of both fuels were calculated to carry an equivalent theoretical number of electrons to the anode. According to theoretical reactions (1) and (2), a 1/6 ratio between ethanol and H_2 was set while keeping a constant total flow rate of 4 L h^{-1} . Therefore, 60% H_2 was switched to 10% ethanol, by controlling the temperature of the thermal bath at 29°C , according to the Clapeyron's law. The inset of Fig. 2 indicated a relatively fast ($t \sim 1.5$ h) stabilization of $i \sim 0.067 \text{ A cm}^{-2}$ at 0.7 V in ethanol. This current density was slightly higher than the one obtained in H_2 ($\sim 0.058 \text{ A cm}^{-2}$). Such a small difference (15%) is related to increased fuel utilization due to a higher global faradic efficiency in ethanol. This observation confirms that reaction (1b) is a simplified view of the complex catalytic and electrochemical processes occurring in the multilayered anode fed directly with ethanol. Nevertheless, this simplified reaction model has to be considered for setting up the experimental flow rates when the fuel is switched from H_2 to ethanol to ensure continuity of the steam release at the anode to assure the gradual internal reforming process.

The most important result of Fig. 2 is the stable operation of the single SOFC under direct anhydrous ethanol for more than 100 h. This is a strong indication that ethanol was converted in the catalytic layer and no carbon reached the Ni. Such a result is supported by previous studies of Ir/ceria catalysts that showed that ethanol is totally converted at 700°C into H_2 (70%), CO (15%), CO_2 (10%), and CH_4 (5%) [22,23]. In addition, previous report of ethanol/water fueled SOFC using ceria-based components confirmed similar ethanol decomposition products by analyzing the gas exit of fuel cells [9]. Moreover, increasing i during fuel cell operation under ethanol/water mixture promoted methane reforming, leading to the conclusion that H_2 was the effective fuel in such conditions [9,17]. Therefore, taken into account that Ir/CGO has been proved as an efficient catalyst for gradual internal reforming of direct methane, the present results strongly suggest that the stable operation of anhydrous ethanol fueled SOFC was based on the same mechanism [15–18]. As compared to the gradual internal reforming of dry methane, similar single fuel cells exhibited a more stable time dependence of the current in ethanol [16–18]. Considering CH_4 steam reforming reaction followed by the electrochemical

oxidation of H_2 [18], a slight current increase was also observed, indicating a better faradaic efficiency using both CH_4 and ethanol than using hydrogen. However, in the case of methane, the absence of a carrier gas significantly changes the residence time of fuel molecules at the surface of the catalyst making further comparisons between direct methane and ethanol fuel cells a difficult task. More importantly, both fuels were found to result in rather stable operation without added water, indicating the flexibility of the studied anode design for different fuels.

As previously mentioned, according to reactions (1) and (2), gradual internal reforming implies in continuous polarization of the fuel cell to ensure continuous steam release while feeding with ethanol. After 65 h of SOFC operation under anhydrous ethanol, the polarization was interrupted for ~ 1 min to investigate the breakdown of the gradual internal reforming mechanism. The interruption of the electrochemical reactions while ethanol was continuously delivered to the fuel cell slightly decreased i to $\sim 0.065 \text{ A cm}^{-2}$ when the polarization was resumed. Such an observation added evidence to the gradual internal reforming, in which the steam produced by the oxidation of the hydrogen plays a major role for ethanol decomposition and stable fuel cell operation. The relatively small decrease of i was not associated with a severe degradation of the properties of the fuel cell. Usually, performance degradation due to carbon formation has been reported to be much more pronounced and to occur faster than the

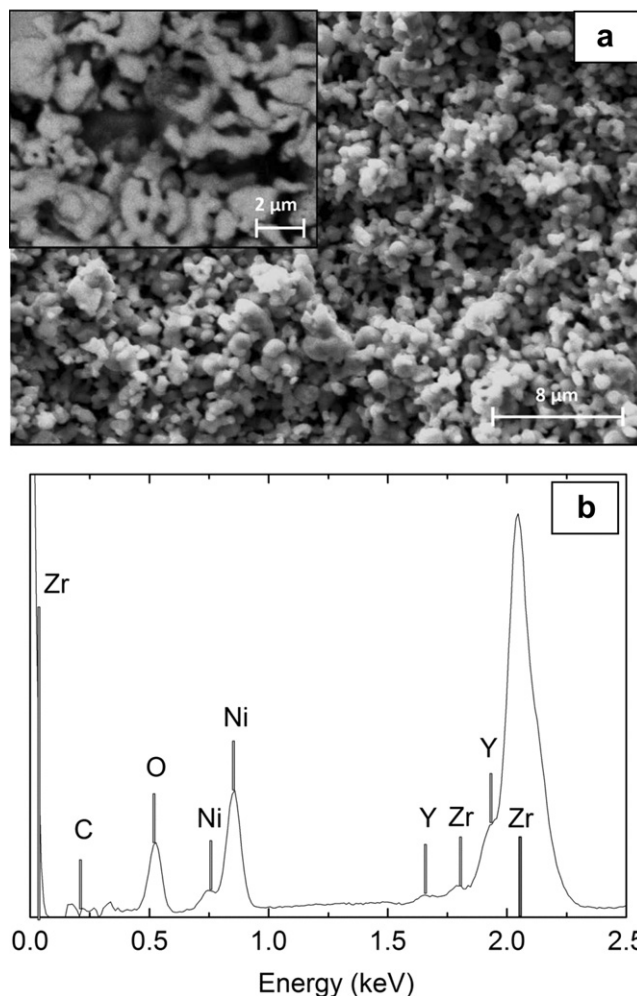


Fig. 3. Scanning electron micrograph (a) and energy dispersive X-ray spectroscopy (b) of the anode after 150 h of operation under anhydrous ethanol.

time interval of the ethanol test shown in Fig. 2 [24]. Nevertheless, the degradation observed for $t > 65$ h is likely to be related to the disruption of the gradual internal reforming, which probably resulted in operation conditions closer to the critical ones for carbon deposition that could deteriorate the catalytic properties of the Ir/CGO layer. This hypothesis is supported by the low performance of the studied cell, in which the fuel utilization was close to the limit at which coking can take place. Nonetheless, further studies are necessary to unveil the details of the ethanol gradual internal reforming mechanism and to disentangle the exact roles played by the properties of the catalytic layer and the Ni/YSZ anode on possible degradation mechanisms. In particular, experiments with practical current densities using high power output anode supported single cells are underway.

After the 150 h test under ethanol, hydrogen was switched back, and EIS was measured, as shown in Fig. 1a. As compared to the initial state, a noticeable increase of both ohmic loss and polarization resistances was measured. Such performance decay was preferably ascribed to an electrochemical degradation due to microstructural evolution of the cell components, which have not been completely optimized. In order to further investigate this point, SEM analyses of the anode were carried out after fuel cell operation to examine possible carbon deposit formation (Fig. 3). Careful SEM and energy dispersive X-ray spectroscopy (EDX) analyses of the anode showed no evidence of carbon deposition, in accordance with the rather stable operation of the SOFC with a carbon containing fuel.

4. Conclusion

In the present study, a SOFC was demonstrated to operate directly with anhydrous ethanol for about 150 h and delivering similar power output as running on hydrogen. The electrochemical characterization indicated that gradual internal steam reforming of sugar cane derived ethanol occurs at the anodic compartment by the addition of a highly catalytically active ceria-based layer onto the anode. The experimental findings shown in this paper,

associated with previous results on dry methane fueled SOFC, suggest that developments of catalytic layers and cell architecture can contribute to the design of multi-fuel SOFCs.

Acknowledgments

Authors are thankful for CAPES-COFECUB, CNPq, CNEN, and ADEME for partial funding and scholarships.

References

- [1] S.C. Singhal, K. Kendall, High Temperature Solid Oxide Fuel Cells, first ed. Elsevier, Oxford, 2003.
- [2] A. Atkinson, S.A. Barnett, R.J. Gorte, J.T.S. Irvine, A.J. McEvoy, M. Mogensen, S.C. Singhal, J.M. Vohs, Nat. Mater. 3 (2004) 17.
- [3] S. McIntosh, R.J. Gorte, Chem. Rev. 104 (2004) 4845–4865.
- [4] S. Park, J.M. Vohs, R.J. Gorte, Nature 404 (2000) 265.
- [5] J. Goldenberg, Science 315 (2007) 808.
- [6] G.A. Deluga, J.R. Salge, L.D. Schmidt, X.E. Verykios, Science 103 (2004) 993.
- [7] B. Huang, X. Zhu, W. Hu, Y. Wang, Q. Yu, J. Power Sources 195 (2010) 3053.
- [8] M. Liao, W. Wang, R. Ran, Z. Shao, J. Power Sources 196 (2011) 6177.
- [9] X.-F. Ye, S.R. Wang, Q. Hu, Z.R. Wang, T.L. Wen, Z.Y. Wen, Electrochem. Commun. 11 (2009) 823.
- [10] X.-F. Ye, S.R. Wang, Q. Hu, J.Y. Chen, T.L. Wen, Z.Y. Wen, Solid State Ionics 180 (2009) 276.
- [11] S. Diethelm, J. Van Herle, J. Power Sources 196 (2010) 7355.
- [12] S.P. Jiang, Y. Ye, T. He, S.B. Ho, J. Power Sources 185 (2008) 179.
- [13] G.P. Corre, J.T.S. Irvine, ECS Trans. 35 (2011) 2845.
- [14] R. Muccillo, E.N.S. Muccillo, F.C. Fonseca, D.Z. de Florio, J. Electrochem. Soc. 155 (2008) B232.
- [15] P. Vernoux, J. Guindet, M. Kleitz, J. Electrochem. Soc. 145 (1998) 3487.
- [16] J.-M. Klein, S. Georges, Y. Bultel, J. Electrochem. Soc. 155 (2008) B333.
- [17] J.-M. Klein, M. Hénault, Y. Bultel, P. Gélin, S. Georges, Electrochem. Solid State Lett. 11 (8) (2008) B144–B147.
- [18] J.-M. Klein, M. Hénault, C. Roux, Y. Bultel, S. Georges, J. Power Sources 193 (2009) 331.
- [19] M. Wisniewski, A. Boréave, P. Gélin, Catal. Commun. 6 (2005) 596.
- [20] W. Wang, Int. J. Hydrogen Energy 36 (2011) 10958.
- [21] Z.L. Zhan, S. Barnett, Solid State Ionics 176 (2005) 871.
- [22] B. Zhang, X. Tang, Y. Li, W. Cai, Y. Xu, W. Shen, Catal. Commun. 7 (2006) 367.
- [23] F. Wang, W. Cai, H. Provendier, Y. Schuurman, C. Descorme, C. Mirodatos, W. Shen, Int. J. Hydrogen Energy 6 (2011) 2.
- [24] C. Mallon, K. Kendall, J. Power Sources 145 (2005) 154–160.